Inorganic Chemistry

Article

pubs.acs.org/IC

Different Factors Govern Chlorination and Encapsulation in Fullerenes: The Case of C_{66}

Núria Alegret, Laura Abella, Khalid Azmani, Antonio Rodríguez-Fortea,* and Josep M. Poblet*

Departament de Química Física i Inorgànica, Universitat Rovira i Virgili, c/Marcel·lí Domingo 1, 43007 Tarragona, Spain

Supporting Information

ABSTRACT: C_{66} is one of the smallest fullerenes that is able to encapsulate more than one metal atom, as in $Sc_2@C_{66}$, as well as to get chlorinated at a low level, $C_{66}Cl_{10}$ or $C_{66}Cl_6$. We show here, with the help of computations at density functional theory level, that these two means of obtaining derivatives of non-isolated pentagon rule fullerenes are dictated by different factors. Chlorination takes place at temperatures lower than 2000 K, once the neutral fullerenes are formed. Encapsulation is, however, mainly governed by the charge transfer, although the Sc···Sc distance is also playing a role in the stability of $Sc_2@C_{66}$.

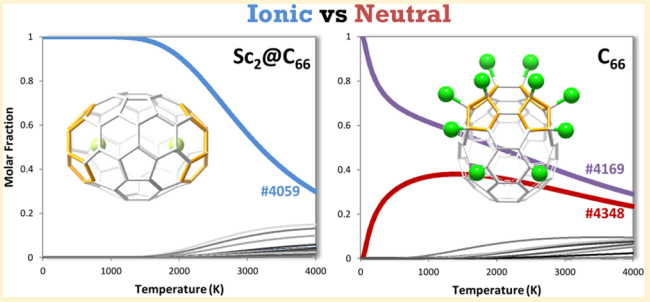

INTRODUCTION

The rule par excellence governing the stability of fullerene cages is the well-known isolated pentagon rule, or IPR, according to which all the cages have the 12 pentagonal rings separated by hexagons.[1,2] The first fullerenes that did not fulfill this rule was reported in the year 2000, with the simultaneous discovery of $Sc_2@C_{66}$ and $Sc_3N@C_{68}$.[3,4] With them, a second factor governing the fullerene's stability emerged: the instability of the non-IPR structures coming from the adjacent pentagons could be counterbalanced by charge transfer from an encapsulated metal atom or cluster.[5−7] Using this approach, many other endohedral non-IPR cages were characterized, such as $Sc_3N@C_{70}$,[8] $La_2@C_{72}$,[9] $Sc_2S@C_{72}$,[10] or $Gd_3N@C_{2n}$ ($2n$ = 78, 82, and 84).[11−14] It was not until 2004, when the first empty non-IPR cage $C_{50}Cl_{10}$ appeared,[15] that a second way of breaking IPR by exohedral derivatization with halogens appeared. Thus, non-IPR fullerenes can be obtained by insertion of metallic clusters inside the cavity or by external addition of halogen (or halogenated) species. Even more, several C_{2n} families ($2n$ = 60, 66, 68, etc.) have been found to show one cage hosting a metal cluster and a different cage exohedrally chlorinated.[16−21]

Among all the non-IPR cages synthesized so far, C_{66} has generated significant controversy in the years since its discovery. In 2000, Shinohara and co-workers synthesized one of the two first non-IPR isomers, with two Sc atoms inside a C_{66} cage. By ^{13}C NMR and synchrotron X-ray powder diffraction analyses, they concluded that the fullerene corresponded to the C_{2v}-$^{\#4348}$ isomer (Figure 1a).[3] However, two years after this first publication, Nagase and co-workers reported a computational study of the same system and, surprisingly, the structure proposed by Shinohara appeared not to be an energy minimum.[22] After an extensive analysis of several orientations of the metal cluster and other possible candidates, they concluded that the most probable cage to encapsulate Sc_2 was the isomer C_{2v}-$^{\#4059}$ (Figure 1b), which completely agreed with the experimental ^{13}C NMR spectrum. This new structure allows a larger separation between the two metal atoms, thus reducing their inherent repulsion present in the first proposal. However, the MEM/Rietveld reanalysis from the X-ray powder diffraction data performed by Shinohara did not match Nagase's choice.[23] The two groups also disagree about the charge transferred from the metal to the cage: Shinohara proposed the system as $Sc_2^{2+}@C_{66}^{2-}$, while Nagase described it as $Sc_2^{6+}@C_{66}^{6-}$.

This controversy about the C_{66} cage was forgotten for several years, and the experimental assignment was generally assumed. However, in 2009 Cui et al. reopened the discussion and, based on theoretical calculations, proposed a third isomer C_2-$^{\#4466}$ to capture Sc_2.[24] As shown in Figure 1c, this new cage has two pairs of adjacent pentagons, as the experimental cage, although its C_2 symmetry satisfied neither the experimental ^{13}C NMR spectra nor the diffraction results.

Later, in 2010, Xie and Zheng reported a new isomer of C_{66} with 6 and 10 chlorine atoms attached on the fullerene surface.[17] This time the cage was undoubtedly characterized with the crystal structure as the $^{\#4169}C_{66}$ isomer (Figure 2a), which was the first fullerene featuring triple sequentially fused pentagons (TSFP). This new characterized isomer, which was different from that assumed to encapsulate two scandiums $Sc_2@^{\#4348}C_{66}$, aroused the curiosity of the fullerene community, and thus, the experiments to chlorinate #4348 isomer started. Recently, Xie and co-workers were able to identify by X-ray crystallography the halogenated $^{\#4348}C_{66}Cl_{10}$, which is shown in Figure 2b.[25] Several months later, Nagase, Akasaka, and co-

Received: May 26, 2015
Published: July 15, 2015

DOI: 10.1021/acs.inorgchem.5b01187
Inorg. Chem. 2015, 54, 7562−7570

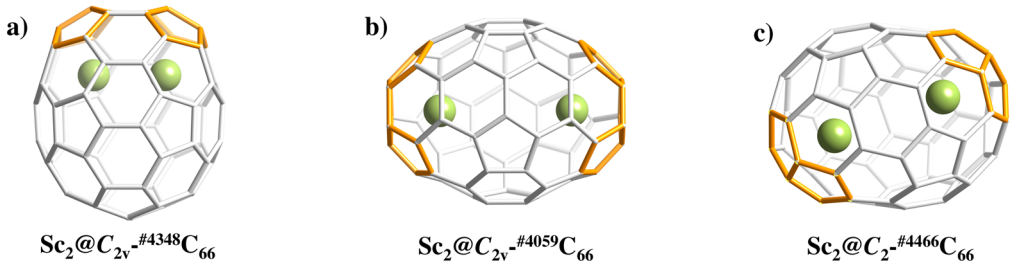

Figure 1. Different cage isomer assignments for $Sc_2@C_{66}$ since its discovery in 2000 (a) Shinohara et al.; (b) Nagase et al.; (c) Cui et al. In orange, the [5,5] pentalene bonds.

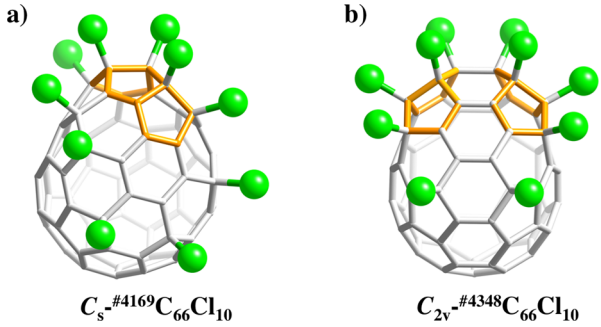

Figure 2. Computed structures of the experimental (a) $^{\#4169}C_{66}Cl_{10}$ and (b) $^{\#4348}C_{66}Cl_{10}$.

workers reported the crystal structure of $Sc_2@^{\#4059}C_{66}$ (Figure 1b), the cage isomer proposed by Nagase in 2002.[26] This is how finally the first experimentally proposed and generally assumed $Sc_2@^{\#4348}C_{66}$ system was discarded.

In summary, three isomers of C_{66} have been observed, two with exohedral derivatization and one with endohedral encapsulation: $^{\#4348}C_{66}Cl_{10}$, $^{\#4169}C_{66}Cl_{10}$, and $^{\#4169}C_{66}Cl_6$, and $Sc_2@^{\#4059}C_{66}$. In this work we tried to understand (i) why endohedral metallofullerenes (EMFs) and exohedrally derivatized fullerenes show different cages; (ii) which is the main property that defines the cage selection in each case; and (iii) predict if any of the isomers could be functionalized in the two different ways.

COMPUTATIONAL DETAILS

All calculations were performed with the combined use of Gaussian09 and ADF-2013. Optimizations of all the empty neutral and anionic cages were performed using semiempirical AM1 calculations with the Gaussian09 code.[27] The most stable neutral and anionic isomers, as well as the EMFs, were recomputed with the DFT BP86/TZP level using the ADF 2013 code.[28] In addition, for the chlorinated species, the Grimme Dispersion D3 method was considered.[29]

To determine the formal charge transfer of the EMFs, orbital analyses were performed, and the results were confirmed by fragment calculations with the ADF-2013 code.[28,30] We defined two fragments: the cluster—Sc_2 or Sc_2C_2—and the empty cage—C_{66} or C_{64}. This fragment option in ADF allows us to tell the program which atoms belongs to each fragment and, therefore, obtain the contribution of each fragment to the molecular orbitals of the whole system.

The vibrational frequencies and the corresponding normal modes were computed using the harmonic approach. Relative abundances along the range of temperatures were obtained from the rigid rotor and harmonic oscillator (RRHO) and the related free-encapsulating model (FEM).[31,32] In the FEM model we consider that if at high temperature the cluster rotates freely inside the cage, its contribution to the partition function will be similar for the different cages and will cancel out.

Molecular dynamics simulations were performed using the Car−Parrinello Molecular Dynamics (CPMD) program.[33,34] The description of the electronic structure was based on the expansion of the valence electronic wave functions into a plane wave basis set, which was limited by an energy cutoff of 40 Ry. The interaction between the valence electrons and the ionic cores was treated through the pseudopotential (PP) approximation (Martins−Troullier type).[35] The functional by Perdew, Burke, and Ernzerhoff (PBE) was selected as density functional,[36,37] and dispersion corrections (Grimme) were included. We used a fictitious electron mass of 800 au. The simulations were performed using periodic boundary conditions in a cubic cell with a side length of 15 Å and a time step of 0.144 fs.

RESULTS AND DISCUSSION

1. Chlorofullerenes. No possible IPR structures exist among the 4478 isomers of C_{66}.[2] In particular, none of them have one pair of fused pentagons (N_p = 1); even more, only three of the isomers have two pentagon adjacencies: #4348 and #4169—both obtained experimentally as halogenated fullerenes (Figure 2)—and #4466—proposed by Cui for $Sc_2@C_{66}$ (Figure 1c). Most of the cages with 66 carbon atoms (176) show four pentagons adjacencies (N_p = 4).

Table 1. Relative Energies, Symmetry, and Number of Adjacent Pentagons (N_p) for the Most Stable Isomers of C_{66} and C_{66}^{6-}

isomer	symmetry	N_p	C_{66} E_{rel}[a] (kcal·mol^{-1})	C_{66}^{6-} E_{rel}[a] (kcal·mol^{-1})
#3764	C_1	3	13.5	14.9
#4007	C_1	3	12.8	28.9
#4059	C_{2v}	4	47.8	1.3
#4169	C_s	2	0.0	26.5
#4348	C_{2v}	2	0.8	18.3
#4398	C_1	3	28.9	2.8
#4407	C_2	4	52.3	6.0
#4410	C_s	3	27.6	2.9
#4417	C_2	4	46.3	0.0
#4437	C_2	4	42.7	3.0
#4454	C_2	3	25.3	2.1
#4466	C_2	2	7.3	21.4

[a]Computed at the BP86/TZP level.

To analyze the chlorine-functionalized fullerenes, we evaluated the 4478 isomers at the neutral state (see Table 1,

DOI: 10.1021/acs.inorgchem.5b01187
Inorg. Chem. 2015, 54, 7562−7570

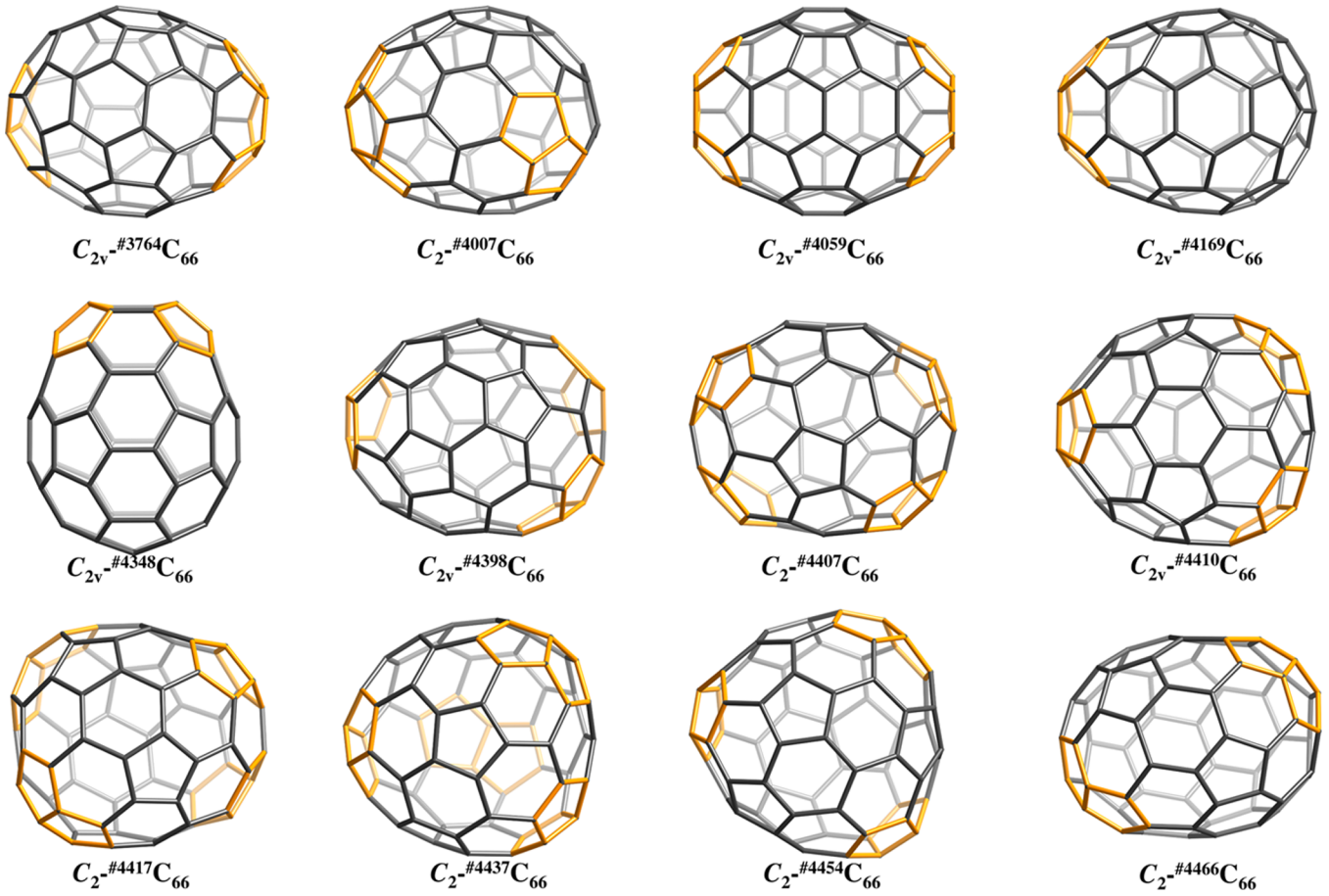

Figure 3. Structures of the 12 C_{66} isomers shown in Table 1.

Figure 3, and Supporting Information). The relative energies of the isomers computed at density functional theory (DFT) level are essentially maintained with respect to the AM1 results. We do not consider the charged species, since there is no electronic transfer present, but covalent bonding between the carbon atoms and the chlorines. The results, Table 1, show that the most stable and almost isoenergetic cages at the neutral state correspond to the two observed chlorinated isomers $^{\#4348}C_{66}$ and $^{\#4169}C_{66}$, followed by isomer $^{\#4466}C_{66}$ at 7.3 kcal·mol^{-1}. All the other isomers appeared at more than 12 kcal·mol^{-1}. Note that the third experimental isomer $^{\#4059}C_{66}$—obtained as an endohedral fullerene—is placed within the first 100 with a relative energy of almost 48 kcal·mol^{-1}. The results confirm that the pentagon adjacency penalty rule (PAPR) applies for the neutral C_{66} isomers (see Supporting Information).[38,39]

The two lowest-energy neutral cages are the ones identified as C_{66} chlorofullerenes. Therefore, we could infer that halogenation took place once the cages are formed. We wonder (i) whether, besides these two cages, other competitive chlorinated fullerenes could be synthesized in the future; and (ii) if isomer $^{\#4059}C_{66}$, the one present in $Sc_2@C_{66}$ with $N_p = 4$ (see Figure 1c), could also be chlorinated. The two low-lying isomers with a set of triple sequentially fused pentagons (TSFP) and one pair of fused pentagons ($N_p = 3$), namely, $^{\#3764}C_{66}$ and $^{\#4007}C_{66}$, were selected as possible candidates to get chlorinated. We considered the halogenated positions of the two experimental systems $^{\#4348}C_{66}$ and $^{\#4169}C_{66}$ as the model to build several $C_{66}Cl_{10}$ isomers and evaluate their energy differences. Structurally, these two fullerenes show $N_p = 2$: $^{\#4348}C_{66}$ has a pair of fused pentagons, while $^{\#4169}C_{66}$ has a single TSFP (Figure 4). From deep analyses of the chlorine positions in these and other non-IPR chlorofullerenes, we confirm that the main rule governing the halogenation is the release of surface strain and that it is structurally achieved through several patterns: (A) several chlorines are placed at the fused pentagons through one [5,5] bond in a zigzag manner, four Cl at the pentalene motif and five at the TSFP; (B) the remaining chlorines are positioned on pentagons near the [5,5] bonds, and, in general, at (1,4) position one from each other; (C) finally, a closed belt of chlorines is formed along the surface.

Taking all these observations into account, we used the $^{\#4059}C_{66}Cl_{10}$ system to validate them and computed 50 different chlorine-patterned regioisomers, collected in the Supporting Infomation. The two most stable regioisomers, separated by 2 kcal·mol^{-1}, satisfy the two conditions A and B: they contain some of the chlorines crossing the two TSFPs, and the remaining chlorines are placed near them, generally at (1,4) positions (see Figure 5). In the case of isomer **1**, the belt of chlorines connects the two TSFP motifs. However, condition C is never achieved in any of the computed regioisomers since there are not enough chlorine atoms to close the belt on the carbon surface. Isomers **3** to **18**, which lie between 6 and 27 kcal·mol^{-1}, were also drawn following the two first observations, although in a way to represent different dispositions to connect the two TSFPs (see Supporting Information). We also confirmed that the patterns designed according to the conditions A and B lead to the most stable structures. For

DOI: 10.1021/acs.inorgchem.5b01187
Inorg. Chem. 2015, 54, 7562−7570

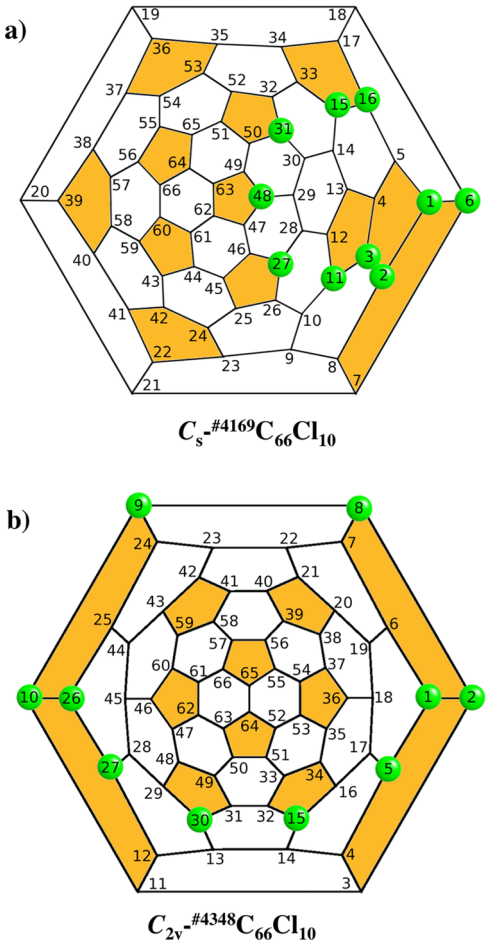

Figure 4. Schlegel diagrams of the two experimental chlorinated fullerenes $^{\#4169}C_{66}Cl_{10}$ (a) and $^{\#4348}C_{66}Cl_{10}$ (b). The pentagons are colored in orange; the positions where the chlorines are attached are highlighted in green.

example, isomers 36 to 46, which contain only two chlorines on the TSFPs and the remaining ones dispersed on the surface, show high relative energies between 100 and 150 kcal·mol^{-1} with respect to the experimental $^{\#4348}C_{66}Cl_{10}$ (see Supporting Information). Besides, isomers 47, 48, and 49, with no chlorines on the pentagon fusions, present relative energies at more than 200 kcal·mol^{-1}. It is worth remarking here that the lowest-energy $^{\#4059}C_{66}Cl_{10}$ isomer **1** still shows much higher energy than the two chlorofullerenes found in experiment, namely, $^{\#4348}C_{66}Cl_{10}$ and $^{\#4169}C_{66}Cl_{10}$.

Once it was verified that the chlorines placed according to the conditions A and B lead to the most stable chloroisomers, we designed the chlorination patterns for isomers #3764, #4007, and #4466 by connecting the two adjacent-pentagon motifs while placing the chlorines at the fused pentagons (condition A) and at the pentagons near them at 1,4 position (condition B). Once again, none of the three isomers reach a number of chlorines sufficient to close the belt around the cage (condition C). A complete list of the energies of the computed isomers can be found in the Supporting Information. At this point, it must be noted that in all the cases studied, including the isomer #4059, the pentagon-fused motifs are not as close as in #4348, and thus there are many possibilities to connect them with chlorines. We found three energy-equivalent chlorine patterns for #4007 within 2 kcal·mol^{-1} of each other; the difference between them is only the position of one of the chlorines (see Figure 6). For isomer #3764, we obtained the most stable regioisomer by almost 4 kcal·mol^{-1}. As mentioned above, isomers #4007 and #3764 have a pentagon pair and a TSFP motif in their carbon structure, so, at first glance, one should expect the same addition pattern for them (see Figure 6). However, the same pattern appears only in the TSFP motifs, with at least four chlorines attached. Isomer #3764 has only two chlorines at the pentagon pair, while the three lowest-energy regiochloroisomers of #4007 have three or four of them. This fact indicates that, when more than one [5,5] bond is present, the relative position of the pentagon-fused motifs, and thus the connection between them by means of chlorines is, in some sense, an important factor that drives the chlorine addition. On the other side, $^{\#4466}C_{66}Cl_{10}$ has also one low-lying regioisomer by 11 kcal·mol^{-1}. Unlike the experimental $^{\#4348}C_{66}Cl_{10}$, only two chlorines are attached at each fused pentagon pair, allowing the structure to release surface strain and connect the two pentalene bonds (see Figure 6). So, once again the relative position of the fused-pentagon junctions plays a key role to determine the number of chlorines attached at each pentagon motif.

Table 2 collects the relative energies of both the experimental and the low-lying computed chloroisomers. As for the neutral pristine cages, the experimental $^{\#4348}C_{66}Cl_{10}$ remains the most stable isomer among all of those calculated. Surprisingly, the second most stable isomer at 8.3 kcal·mol^{-1} is the computed $^{\#4466}C_{66}Cl_{10}$. Above them, between 19.5 and 23.6 kcal·mol^{-1} a set of chlorofullerenes includes the $^{\#3764}C_{66}Cl_{10}$, the experimental $^{\#4169}C_{66}Cl_{10}$, and the regioisomers of $^{\#4007}C_{66}Cl_{10}$. Quite higher, the $^{\#4059}C_{66}Cl_{10}$ lays at more than 38 kcal·mol^{-1}. Such results are not conclusive enough to discard the possible formation of other $C_{66}Cl_{10}$ species. For that reason, we also evaluated the molar fractions of the lowest-energy isomers as a function of the temperature. We used the rigid rotor and harmonic oscillator (RRHO) approximation.[31,32] As shown in Figure 7, the C_{2v}-$^{\#4348}C_{66}Cl_{10}$ is the most abundant chlorofullerene up to 1000 K. At 2000 K and higher temperatures, isomer $^{\#4466}C_{66}Cl_{10}$ achieves abundances up to 80%. The remaining isomers increase slightly their relative abundances with the temperature, although none of them exceed the 10%. It is surprising that, according to these results, the experimentally synthesized $^{\#4169}C_{66}Cl_{10}$ should have never been obtained, and that $^{\#4466}C_{66}Cl_{10}$ should be observed instead. This could indicate either that isomer $^{\#4466}C_{66}Cl_{10}$ is also feasible for halogenation, and it will be synthesized, or that the halogenation of the cages takes place at relatively low temperatures; thus, the principal driving force to produce halogenated species is the formation of the pristine cages—note that the experimental $^{\#4348}C_{66}$ and $^{\#4169}C_{66}$ isomers are the most abundant neutral cages in the whole range of temperatures as shown in Figure 7. We are currently performing further studies in this direction.

Car−Parrinello molecular dynamics (MD) simulations were also performed to provide more insight into the motion of chlorines at high temperatures. The trajectories at 2000 K for the experimental C_{2v}-$^{\#4348}C_{66}Cl_{10}$ cage show that chlorine atoms are lost after the first 4 ps. This result indicates that chlorination of fullerenes does not take place at 2000 K but at lower temperatures. Trajectories at 1000 and 800 K confirm that chlorines remain at their original positions at the rather short time scale simulated here (~50 ps), as shown in Figure 8. Detachment and subsequent attachment of a single chlorine

DOI: 10.1021/acs.inorgchem.5b01187
Inorg. Chem. 2015, 54, 7562−7570

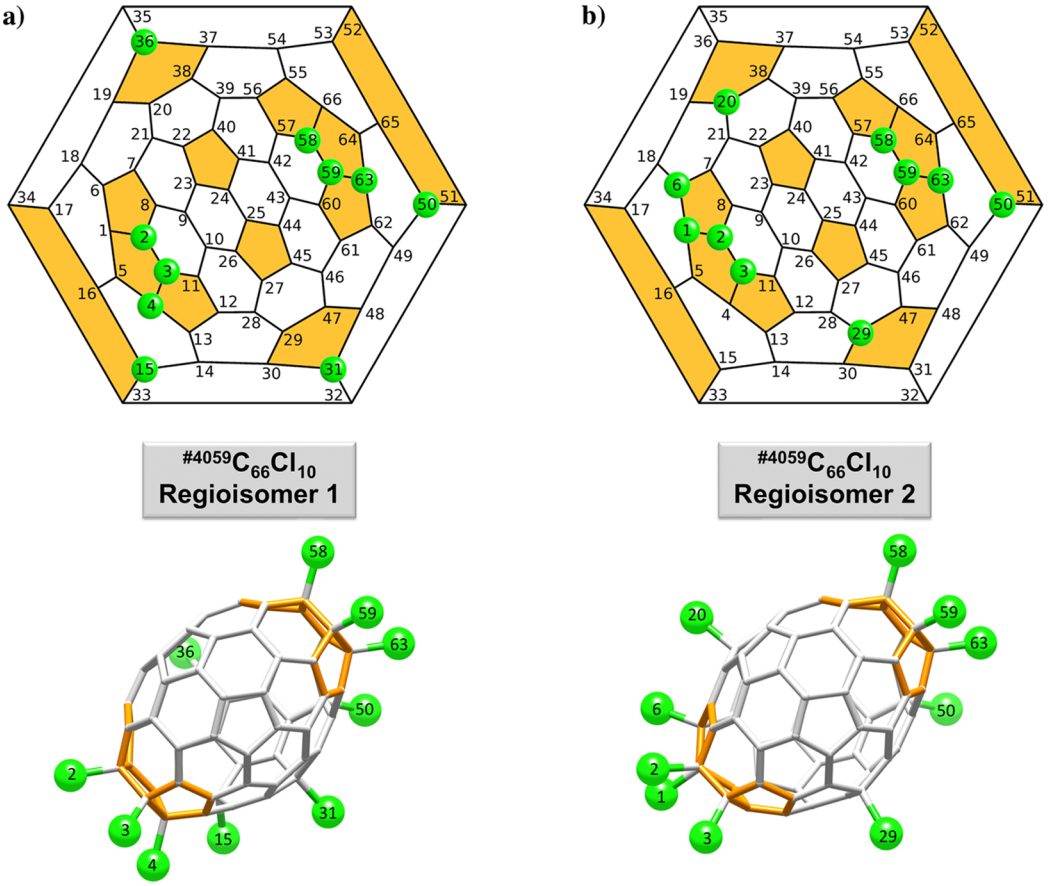

Figure 5. Schlegel diagrams of the two lowest-energy chlorinated structures for the $^{\#4059}C_{66}Cl_{10}$ system. The pentagons are colored in orange; the positions where the chlorines are attached are highlighted in green.

atom are rarely observed in some of these simulations, keeping the fullerene the total number of chlorines at the end of the trajectories. Therefore, chlorination is expected once the temperature in the arc is reduced (much lower than 2000 K) and the empty cages formed.

2. Endohedral $Sc_2@C_{66}$ Isomers. Since the discovery of one of the first non-IPR fullerenes $Sc_2@C_{66}$, a lot has been speculated about the carbon cage that encapsulates the dimetallic cluster. First, Shinohara proposed the isomer C_{2v}-$^{\#4348}$, based on experimental data; later, Nagase demonstrated that this first guess did not correspond to the thermodynamically favorable isomer, so he proposed cage C_{2v}-$^{\#4059}$ to encapsulate the two Sc atoms. Fourteen years after the first detection of $Sc_2@C_{66}$, the crystal structure was finally resolved as $Sc_2@^{\#4059}C_{66}$. There might be still a thought that the experiments performed in the years 2000 and 2014 to synthesize $Sc_2@C_{66}$ do not lead to the same fullerene mixture and each isomer, namely, C_{2v}-$^{\#4348}$ and C_{2v}-$^{\#4059}$, can be found experimentally. Here we confirm that the most likely cage for $Sc_2@C_{66}$ is the C_{2v}-$^{\#4059}$ isomer. In addition, we demonstrate that there is a formal transfer of six electrons from the encapsulated atoms to the carbon cage, $(Sc_2)^{6+}@C_{66}{}^{6-}$, and that the minimization of electrostatic repulsion between the two Sc^{3+} ions is playing a major role in the final selection of cage C_{2v}-$^{\#4059}$.

To evaluate which isomer better fits the requirement to encapsulate the Sc atoms, we take into account the ionic model and make the preliminary assumption (which is later confirmed, vide infra) that there is a formal transfer of six electrons from the metal atoms to the carbon cage. Thus, we analyzed *all* the 4478 hexa-anionic cages at semiempirical (AM1) level and then recomputed the lowest-energy isomers at DFT level (see Computational Details). The results collected in Table 1 show that the isomers are much closer in energy than in the neutral state. The most stable hexa-anionic isomer is $^{\#4417}C_{66}{}^{6-}$, followed by $^{\#4059}C_{66}{}^{6-}$ at 1.3 kcal·mol^{-1}. Above them, the cages #4454, #4398, and #4410 appeared in the range of 2−3 kcal·mol^{-1}, and the #4407 at 6 kcal·mol^{-1}. Finally, the most stable neutral isomers #4348, #4169, #4466, #3764, and #4007 lie at more than 15 kcal·mol^{-1}.

To include the metal−pentalene interaction effect,[40] as well as the electrostatic repulsion between the Sc^{3+} ions, we computed the endohedral species for the most stable empty C_{66} hexa-anionic cages and the ones under discussion. To optimize the electrostatic interactions, both between the metals and the pentalenes and between metal ions, we placed the Sc atoms near the pentagon junctions and as much separated as possible between them. Results collected in Table 3 show that the encapsulation of the cluster produces higher energy differences among isomers, when compared to the hexa-anionic systems, due mainly to the different Sc···Sc distances and, to a lesser extent, to the slightly different metal−pentalene interaction in each isomer. All the optimized structures are represented in Figure 9. Isomer #4059 is by far the most stable one, in agreement with the work of Nagase, and the remaining ones appear at more than 22 kcal·mol^{-1}. Note that isomer #4417, which was isoenergetic to the #4059 isomer in the hexa-anionic state, is found at 28 kcal·mol^{-1}, whereas cage #4348 lies

DOI: 10.1021/acs.inorgchem.5b01187
Inorg. Chem. 2015, 54, 7562−7570

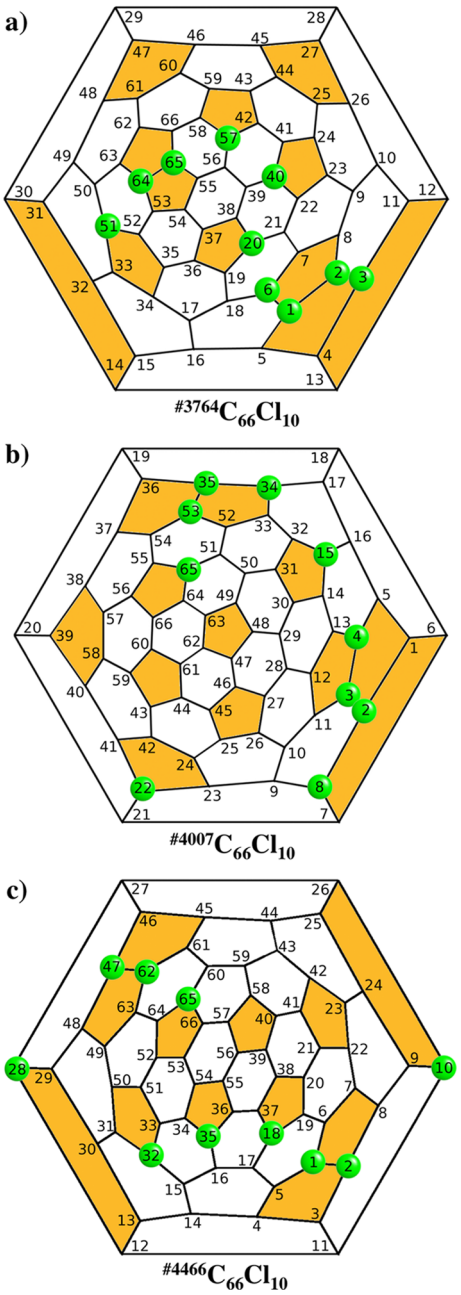

Figure 6. Schlegel diagram of the most stable chlorinated structure for (a) $^{\#3764}C_{66}Cl_{10}$, (b) $^{\#4007}C_{66}Cl_{10}$, and (c) $^{\#4466}C_{66}Cl_{10}$. The pentagons are colored in orange; the positions where the chlorines are attached are highlighted in green.

Table 2. Relative Energies for the Lowest $C_{66}Cl_{10}$ Isomers

$C_{66}Cl_{10}$ isomer	E_{rel} (kcal·mol^{-1})
#4348	0.0
#4466	8.3
#3764	19.5
#4169	21.1
#4007−1	21.6
#4007−2	21.8
#4007−3	23.6
#4059−1	38.7
#4059−2	40.7

almost at 80 kcal·mol^{-1}. According to Nagase,[22] the endohedral $Sc_2@^{\#4348}C_{66}$, as described by Shinohara and drawn in Figure 1, does not appear as a minimum in the potential energy surface since the repulsion between the two Sc atoms is too high—the distance between Sc atoms is ∼2.7 Å inside the $^{\#4348}C_{66}$ cage, while it increases to 4.92 Å in the #4059 isomer. Nagase also analyzed other conformations of the scandium ions inside the #4348 cage and concluded that a rotation of 90° of the Sc_2 results in an energy minimum. This orientation is labeled in Table 3 and Figure 9 as isomer #4348 (minimum). According to our results, which agree completely with those obtained by Nagase, such a simple rotation decreases the energy of the endofullerene by 40 kcal·mol^{-1}, due to the increase of the distance between the Sc^{3+} ions to 4.05 Å and, thus, a reduction of their repulsion. However, this decrease is not enough to reverse energies with the most stable cage #4059.

In general, we observe that the higher the repulsion between the Sc atoms, that is, the shorter the Sc···Sc distance, the lower the stability of the whole system (see Figure 10). Since the metal ions carry considerable positive charge, the repulsive electrostatic interaction between them is rather strong, as pointed out by Nagase[22] and also seen in other works with dimetallic endofullerenes, such as $La_2@D_{2h}$-C_{80}.[41] Therefore, we confirm that one important factor that drives the stability of these endofullerenes is the Sc···Sc separation; see Figure S8 for a plot of the relative energies of the $Sc_2@C_{66}$ isomers as a function of the Sc···Sc distances. If we assume that the relative stabilization of EMFs ΔE comes from (i) the stabilities of the anionic cages (ionic model), ΔE_{ionic}, and (ii) the presence of the metals in the cage, an even better correlation is found when we plot $\Delta E - \Delta E_{ionic}$ against the Sc···Sc distances, that is, subtract from the relative energies the contribution from the ionic model; see Figure 10.

Even though $Sc_2@^{\#4059}C_{66}$ is by difference the lowest-energy isomer, we also analyzed the effect that the high-temperature conditions in which fullerenes are synthesized can have in the relative stability of the isomers. The predicted free energy and molar fractions up to 4000 K confirm that $Sc_2@^{\#4059}C_{66}$ is the most abundant and the only isomer with appreciable molar fraction for the whole range of temperature (Figure 11). We completed the study considering the family of the carbide $Sc_2C_2@C_{64}$ clusterfullerenes, which share the same Sc_2C_{66} stoichiometry with the metal endofullerenes $Sc_2@C_{66}$. The rather high relative energies at 0 K for the lowest-energy carbides compared to $Sc_2@^{\#4059}C_{66}$ (see Supporting Information), as well as the negligible molar fractions up to 4000 K, clearly discard this possibility.

Finally, the formal charge transfer was determined by means of molecular orbital interaction diagrams of the two fragments Sc_2 and C_{66}. The orbital diagram for the #4059 structure is represented in Figure 12 (the diagrams for other isomers are collected in the Supporting Information). Figure 12 clearly shows that the highest occupied molecular orbital (HOMO), HOMO−1, and HOMO−2 of the Sc_2 fragment (green in Figure 12) transfer their six electrons to the three lowest unoccupied molecular orbitals (LUMOs) of the cage, namely, LUMO, LUMO+1, and LUMO+2 (gray in Figure 12). Thus, these three orbitals of the C_{66} cage become the HOMO, HOMO−1, and HOMO−2 of the endofullerene (green arrows in Figure 12), while the HOMO−2 of the metal fragment becomes the LUMO of $Sc_2@^{\#4059}C_{66}$, as shown with dashed lines in Figure 12. Similar results were obtained for all the other endofullerenes analyzed here, including the #4348 isomer with

DOI: 10.1021/acs.inorgchem.5b01187
Inorg. Chem. 2015, 54, 7562−7570

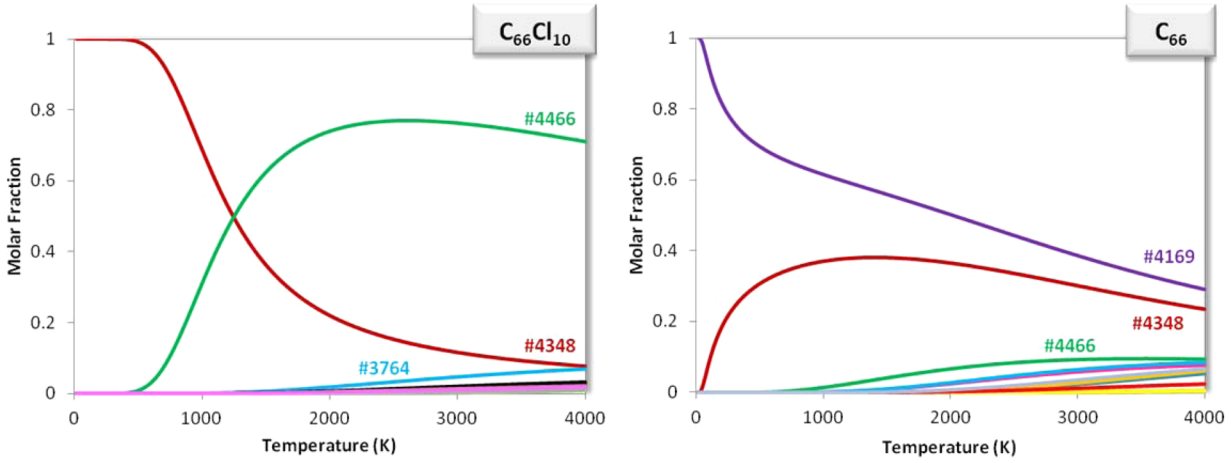

Figure 7. Representation of the molar fraction as a function of the temperature for the isomers of $C_{66}Cl_{10}$ and C_{66} using the RRHO approximation. Only the three most abundant isomers are labeled (see the Supporting Information for a complete description).

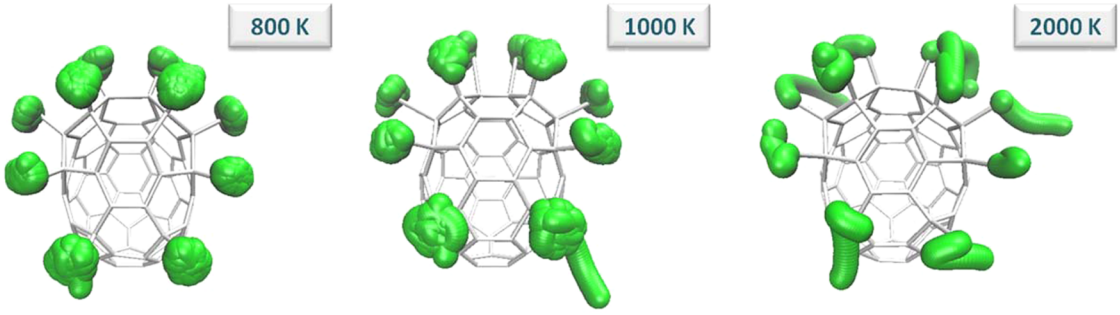

Figure 8. Representation of the motion of the Cl atoms in C_{2v}-$^{\#4348}C_{66}Cl_{10}$ during Car–Parrinello MD trajectories at 800, 1000, and 2000 K.

Table 3. Relative Energies with the Formal Electron Transfers and the Sc···Sc Distances for Specific $Sc_2@C_{66}$ Fullerene Isomers

isomer	E_{rel}[a] (kcal·mol^{-1})	formal transfer	Sc···Sc (Å)
#4059	0.0	6–	4.92
#4398	22.0	6–	4.34
#4410	23.6	6–	4.06
#3764	25.8	6–	4.47
#4407	27.2	6–	4.26
#4417	28.0	6–	3.87
#4454	28.4	6–	3.78
#4169	29.6	4–	3.31
#4437	32.7	6–	3.57
#4348 (minimum)	38.0	6–	4.05
#4007	38.6	6–	3.65
#4466	40.1	6–	4.11
#4348	81.3	4–	2.69

[a]Computed at the BP86/TZP level.

the cluster in vertical position (the minimum), except for the $Sc_2@C_{2v}$-$^{\#4348}C_{66}$ and $Sc_2@C_{2v}$-$^{\#4169}C_{66}$. For these latter systems, the Sc_2 cluster transfers only four electrons to the carbon cage (see Supporting Information). A correlation with the Sc···Sc distances exists: the shorter the distance, the stronger the covalent Sc–Sc bond and, therefore, the lower the number of transferred electrons. Even though the usual transfer of Sc-based clusters is three electrons per metal, it is not surprising that these two endofullerenes with the shortest Sc–Sc distances—2.7 Å for the #4348 isomer and 3.3 Å for #4169—transfer only four electrons.

CONCLUSIONS

Exohedral as well as endohedral derivatives are found in the C_{66} fullerene family, but those isomers that get chlorinated ($^{\#4348}C_{66}$, $^{\#4169}C_{66}$) are not able to encapsulate metal atoms ($^{\#4059}C_{66}$) and vice versa. According to our results, low-energy neutral cages are the ones that are functionalized when a chlorine source is introduced in the arc. Chlorination would take place at a temperature significantly lower than 2000 K, once the neutral isomers were formed. Chlorination patterns follow the trend of maximizing strain release on the cage surface, with chlorines at the highly pyramidalized C atoms of the adjacent pentagons. In addition, the relative position of the adjacent pentagons may also play a role. Thus, besides $^{\#4348}C_{66}$ and $^{\#4169}C_{66}$, cage $^{\#4466}C_{66}$ with two adjacent pentagon pairs could also be detected as chlorofullerene in the future.

Alternatively, the stability of endohedral $Sc_2@C_{66}$ is given by (i) the electron transfer from the metal atoms to the cage (ionic model); (ii) the interaction between the Sc and the cage; and (iii) the interaction between the two Sc ions. After exhaustive exploration, $Sc_2@^{\#4059}C_{66}$ is found to be the most abundant cage for the whole range of temperatures, as proposed by Nagase and recently confirmed by X-ray diffraction experiments. Isomer $Sc_2@^{\#4398}C_{66}$ might also be detected. For the lowest-energy EMFs, formal transfer of six electrons is found, $Sc_2^{6+}@C_{66}^{6-}$, with no covalent bond between the two Sc ions. Besides the stability given by the electron transfer, electrostatic

DOI: 10.1021/acs.inorgchem.5b01187
Inorg. Chem. 2015, 54, 7562–7570

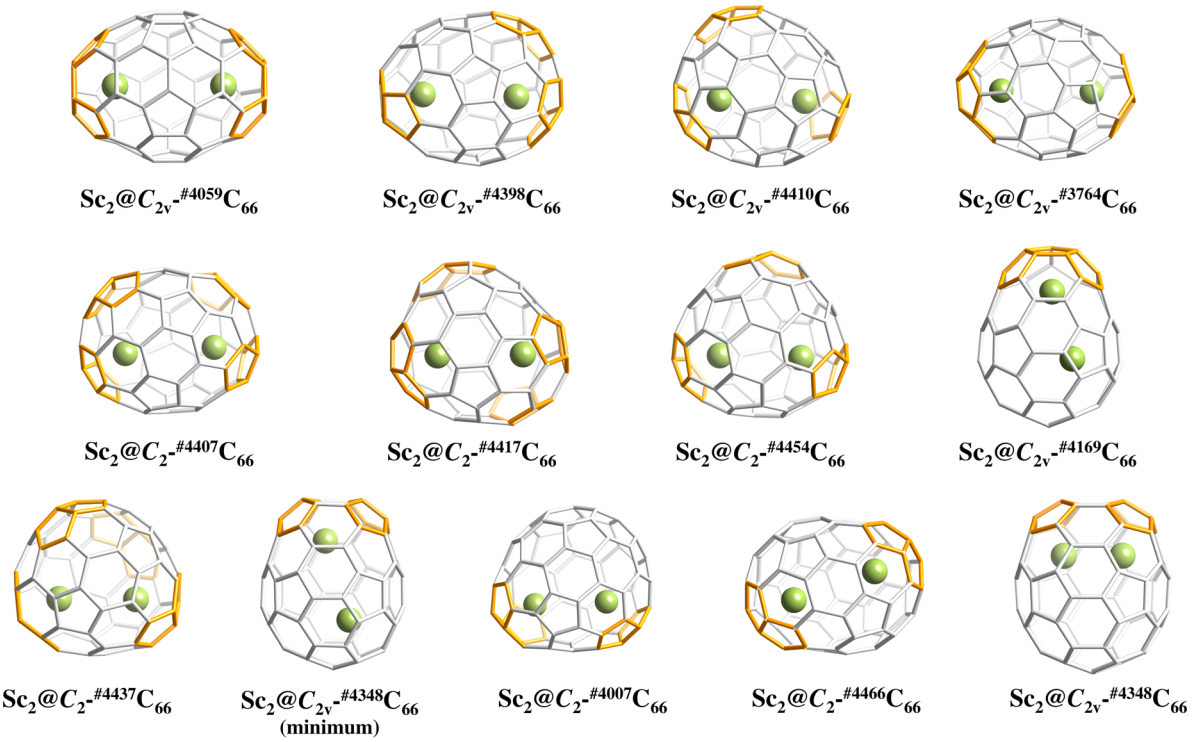

Figure 9. Optimized structures of the computed $Sc_2@C_{66}$ systems in Table 3.

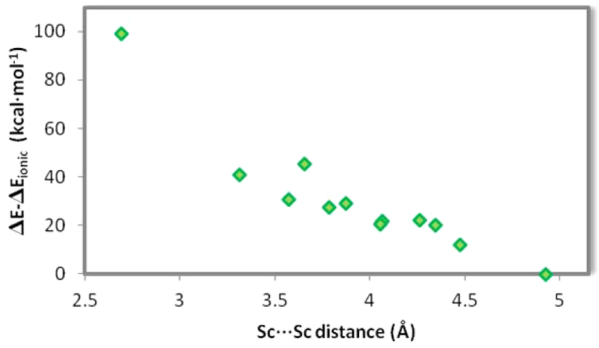

Figure 10. Relative energies of the $Sc_2@C_{66}$ isomers when subtracting the contribution from the ionic model, $\Delta E - \Delta E_{ionic}$ (see text), as a function of the Sc···Sc distance.

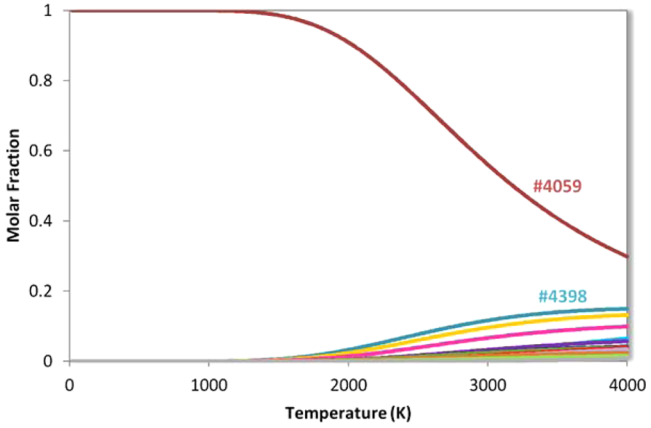

Figure 11. Predicted molar fractions for the lowest-energy $Sc_2@C_{66}$ isomers as a function of temperature. The lowest-energy carbide $Sc_2C_2@C_{64}$ clusterfullerene was also considered. Only the two most abundant isomers are labeled (see the Supporting Information for a complete description).

repulsion between Sc^{3+} ions sets the stability trends of $Sc_2@C_{66}$ endofullerenes.

■ ASSOCIATED CONTENT

Supporting Information

Relative energies and structures of a larger list of $C_{66}Cl_{10}$ and $Sc_2@C_{66}$ isomers, as well as their abundances and orbital interaction diagrams for some of the EMFs. The Supporting Information is available free of charge on the ACS Publications website at DOI: 10.1021/acs.inorgchem.5b01187.

■ AUTHOR INFORMATION

Corresponding Authors

*E-mail: antonio.rodriguezf@urv.cat. (A.R.F.)
*E-mail: josepmaria.poblet@urv.cat. (J.M.P.)

Notes

The authors declare no competing financial interest.

■ ACKNOWLEDGMENTS

This work was supported by the Spanish Ministerio de Ciencia e Innovación (Project No. CTQ2014-52774-P) and by the Generalitat de Catalunya (Nos. 2014SGR-199 and XRQTC). L.A. thanks the Generalitat de Catalunya for a predoctoral fellowship (No. FI-DGR 2014).

■ REFERENCES

(1) Kroto, H. W. *Nature* **1987**, *329*, 529.
(2) Fowler, P. W.; Manolopoulos, D. E. *An Atlas of Fullerenes;* Oxford University Press: Oxford, U.K., 1995.
(3) Wang, C.; Kai, T.; Tomiyama, T.; Yoshida, T.; Kobayashi, Y.; Nishibori, E.; Takata, M.; Sakata, M.; Shinohara, H. *Nature* **2000**, *408*, 426.

DOI: 10.1021/acs.inorgchem.5b01187
Inorg. Chem. 2015, 54, 7562−7570

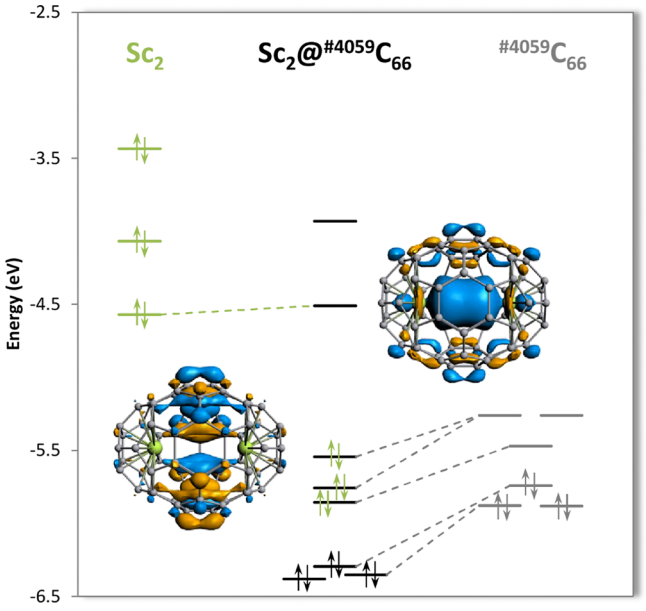

Figure 12. Molecular orbital diagram that shows the formal transfer of six electrons in $Sc_2@C_{2v}$-$^{\#4059}C_{66}$. In green, the Sc_2 fragment; in gray, the C_{66} fragment; in black, $Sc_2@C_{66}$. The HOMO and the LUMO of $Sc_2@C_{2v}$-$^{\#4059}C_{66}$ are also represented.

(4) Stevenson, S.; Fowler, P. W.; Heine, T.; Duchamp, J. C.; Rice, G.; Glass, T.; Harich, K.; Hajdu, E.; Bible, R.; Dorn, H. C. *Nature* **2000**, *408*, 427.
(5) Popov, A.; Yang, S.; Dunsch, L. *Chem. Rev.* **2013**, *113*, 5989.
(6) Rodríguez-Fortea, A.; Balch, A.; Poblet, J. *Chem. Soc. Rev.* **2011**, *40*, 3551.
(7) Rodríguez-Fortea, A.; Alegret, N.; Balch, A. L.; Poblet, J. M. *Nat. Chem.* **2010**, *2*, 955.
(8) Yang, S.; Popov, A.; Dunsch, L. *Angew. Chem., Int. Ed.* **2007**, *46*, 1256.
(9) Lu, X.; Nikawa, H.; Nakahodo, T.; Tsuchiya, T.; Ishitsuka, M. O.; Maeda, Y.; Akasaka, T.; Toki, M.; Sawa, H.; Slanina, Z.; Mizorogi, N.; Nagase, S. *J. Am. Chem. Soc.* **2008**, *130*, 9129.
(10) Chen, N.; Beavers, C.; Mulet-Gas, M.; Rodríguez-Fortea, A.; Munoz, E.; Li, Y.-Y.; Olmstead, M.; Balch, A.; Poblet, J.; Echegoyen, L. *J. Am. Chem. Soc.* **2012**, *134*, 7851.
(11) Alegret, N.; Chaur, M. N.; Santos, E.; Rodriguez-Fortea, A.; Echegoyen, L.; Poblet, J. M. *J. Org. Chem.* **2010**, *75*, 8299.
(12) Mercado, B. Q.; Beavers, C. M.; Olmstead, M. M.; Chaur, M. N.; Walker, K.; Holloway, B. C.; Echegoyen, L.; Balch, A. L. *J. Am. Chem. Soc.* **2008**, *130*, 7854.
(13) Beavers, C. M.; Chaur, M. N.; Olmstead, M. M.; Echegoyen, L.; Balch, A. L. *J. Am. Chem. Soc.* **2009**, *131*, 11519.
(14) Zuo, T.; Walker, K.; Olmstead, M. M.; Melin, F.; Holloway, B. C.; Echegoyen, L.; Dorn, H. C.; Chaur, M. N.; Chancellor, C. J.; Beavers, C. M.; Balch, A. L.; Athans, A. J. *Chem. Commun.* **2008**, 1067.
(15) Xie, S.-Y.; Gao, F.; Lu, X.; Huang, R.-B.; Wang, C.-R.; Zhang, X.; Liu, M.-L.; Deng, S.-L.; Zheng, L.-S. *Science* **2004**, *304*, 699.
(16) Tan, Y.-Z.; Chen, R.-T.; Liao, Z.-J.; Li, J.; Zhu, F.; Lu, X.; Xie, S.-Y.; Li, J.; Huang, R.-B.; Zheng, L.-S. *Nat. Commun.* **2011**, *2*, 420.
(17) Tan, Y.-Z.; Li, J.; Zhu, F.; Han, X.; Jiang, W.-S.; Huang, R.-B.; Zheng, Z.; Qian, Z.-Z.; Chen, R.-T.; Liao, Z.-J.; Xie, S.-Y.; Lu, X.; Zheng, L.-S. *Nat. Chem.* **2010**, *2*, 269.
(18) Tan, Y.-Z.; Liao, Z.-J.; Qian, Z.-Z.; Chen, R.-T.; Wu, X.; Liang, H.; Han, X.; Zhu, F.; Zhou, S.-J.; Zheng, Z.; Lu, X.; Xie, S.-Y.; Huang, R.-B.; Zheng, L.-S. *Nat. Mater.* **2008**, *7*, 790.
(19) Tan, Y.-Z.; Zhou, T.; Bao, J.; Shan, G.-J.; Xie, S.-Y.; Huang, R.-B.; Zheng, L.-S. *J. Am. Chem. Soc.* **2010**, *132*, 17102.
(20) Simeonov, K. S.; Amsharov, K. Y.; Jansen, M. *Chem. - Eur. J.* **2008**, *14*, 9585.
(21) Han, X.; Zhou, S.-J.; Tan, Y.-Z.; Wu, X.; Gao, F.; Liao, Z.-J.; Huang, R.-B.; Feng, Y.-Q.; Lu, X.; Xie, S.-Y.; Zheng, L.-S. *Angew. Chem., Int. Ed.* **2008**, *47*, 5340.
(22) Kobayashi, K.; Nagase, S. *Chem. Phys. Lett.* **2002**, *362*, 373.
(23) Masaki, T.; Nishibori, E.; Sakata, M.; Wang, C. R.; Shinohara, H. *Chem. Phys. Lett.* **2003**, *372*, 512.
(24) Cui, Y. H.; Tian, W. Q.; Feng, J. K.; Chen, D. L. *J. Nanopart. Res.* **2010**, *12*, 429.
(25) Gao, C.-L.; Li, X.; Tan, Y.-Z.; Wu, X.-Z.; Zhang, Q.; Xie, S.-Y.; Huang, R.-B. *Angew. Chem., Int. Ed.* **2014**, *53*, 7853.
(26) Yamada, M.; Kurihara, H.; Suzuki, M.; Guo, J. D.; Waelchli, M.; Olmstead, M. M.; Balch, A. L.; Nagase, S.; Maeda, Y.; Hasegawa, T.; Lu, X.; Akasaka, T. *J. Am. Chem. Soc.* **2014**, *136*, 7611.
(27) Frisch, M. J.; Trucks, G. W.; Schlegel, H. B.; Scuseria, G. E.; Robb, M. A.; Cheeseman, J. R.; Scalmani, G.; Barone, V.; Mennucci, B.; Petersson, G. A.; Nakatsuji, H.; Caricato, M.; Li, X.; Hratchian, H. P.; Izmaylov, A. F.; Bloino, J.; Zheng, G.; Sonnenberg, J. L.; Hada, M.; Ehara, M.; Toyota, K.; Fukuda, R.; Hasegawa, J.; Ishida, M.; Nakajima, T.; Honda, Y.; Kitao, O.; Nakai, H.; Vreven, T.; Montgomery, J. A., Jr.; Peralta, J. E.; Ogliaro, F.; Bearpark, M.; Heyd, J. J.; Brothers, E.; Kudin, K. N.; Staroverov, V. N.; Kobayashi, R.; Normand, J.; Raghavachari, K.; Rendell, A.; Burant, J. C.; Iyengar, S. S.; Tomasi, J.; Cossi, M.; Rega, N.; Millam, J. M.; Klene, M.; Knox, J. E.; Cross, J. B.; Bakken, V.; Adamo, C.; Jaramillo, J.; Gomperts, R.; Stratmann, R. E.; Yazyev, O.; Austin, A. J.; Cammi, R.; Pomelli, C.; Ochterski, J. W.; Martin, R. L.; Morokuma, K.; Zakrzewski, V. G.; Voth, G. A.; Salvador, P.; Dannenberg, J. J.; Dapprich, S.; Daniels, A. D.; Farkas, Ö.; Foresman, J. B.; Ortiz, J. V.; Cioslowski, J.; Fox, D. J. *Gaussian09;* Gaussian, Inc: Wallingford, CT, 2009.
(28) Baerends, E. J.; Ellis, D. E.; Ros, P. *ADF 2013.01;* SCM: Amsterdam, 2008.
(29) Grimme, S.; Antony, J.; Ehrlich, S.; Krieg, H. *J. Chem. Phys.* **2010**, *132*, 154104.
(30) Velde, G. t.; Bickelhaupt, F. M.; Baerends, E. J.; Guerra, C. F.; Gisbergen, S. J. A. v.; Snijders, J. G.; Ziegler, T. *J. Comput. Chem.* **2001**, *22*, 932.
(31) Slanina, Z.; Nagase, S. *ChemPhysChem* **2005**, *6*, 2060.
(32) Slanina, Z.; Lee, S. L.; Uhlík, F.; Adamowicz, L.; Nagase, S. *Theor. Chem. Acc.* **2007**, *117*, 315.
(33) Car, R.; Parrinello, M. *Phys. Rev. Lett.* **1985**, *55*, 2471.
(34) *CPMD*, v3.15; copyright held jointly by Max Planck Institute and IBM Corp., Stuttgart, Germany, 1997−2001; http://cpmd.org/download.
(35) Troullier, N.; Martins, J. L. *Phys. Rev. B: Condens. Matter Mater. Phys.* **1991**, *43*, 1993.
(36) Perdew, J. P.; Burke, K.; Ernzerhof, M. *Phys. Rev. Lett.* **1996**, *77*, 3865.
(37) Perdew, J. P.; Burke, K.; Ernzerhof, M. *Phys. Rev. Lett.* **1997**, *78*, 1396.
(38) Campbell, E. E. B.; Fowler, P. W.; Mitchell, D.; Zerbetto, F. *Chem. Phys. Lett.* **1996**, *250*, 544.
(39) Albertazzi, E.; Domene, C.; Fowler, P. W.; Heine, T.; Seifert, G.; Van Alsenoy, C.; Zerbetto, F. *Phys. Chem. Chem. Phys.* **1999**, *1*, 2913.
(40) Tan, Y. Z.; Xie, S. Y.; Huang, R. B.; Zheng, L. S. *Nat. Chem.* **2009**, *1*, 450.
(41) Popov, A. A.; Dunsch, L. *Chem. - Eur. J.* **2009**, *15*, 9707.

DOI: 10.1021/acs.inorgchem.5b01187
Inorg. Chem. 2015, 54, 7562−7570